

Supplementary material

SiO_x Anode Strengthened by Self-Catalytic Growth of Carbon Nanotubes

Hongjin Xue,^{a,b} Yong Cheng,^{a*} Qianqian Gu,^{a,b} Zhaomin Wang,^a Yabin Shen,^{a,b} Dongming Yin,^{a,b} Limin Wang^{a,b} and Gang Huang^{a*}

^a State Key Laboratory of Rare Earth Resource Utilization, Changchun Institute of Applied Chemistry Chinese Academy of Sciences, Changchun, 130022, China

^b University of Science and Technology of China, Hefei, 230026, China

*Address correspondence to: cyong@ciac.ac.cn; gchuang@ciac.ac.cn.

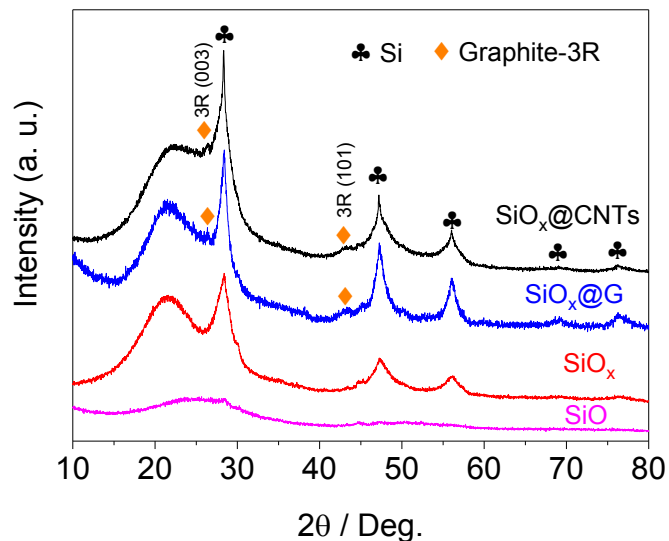


Figure S1. XRD patterns of SiO, SiO_x, SiO_x@G, and SiO_x@CNTs.

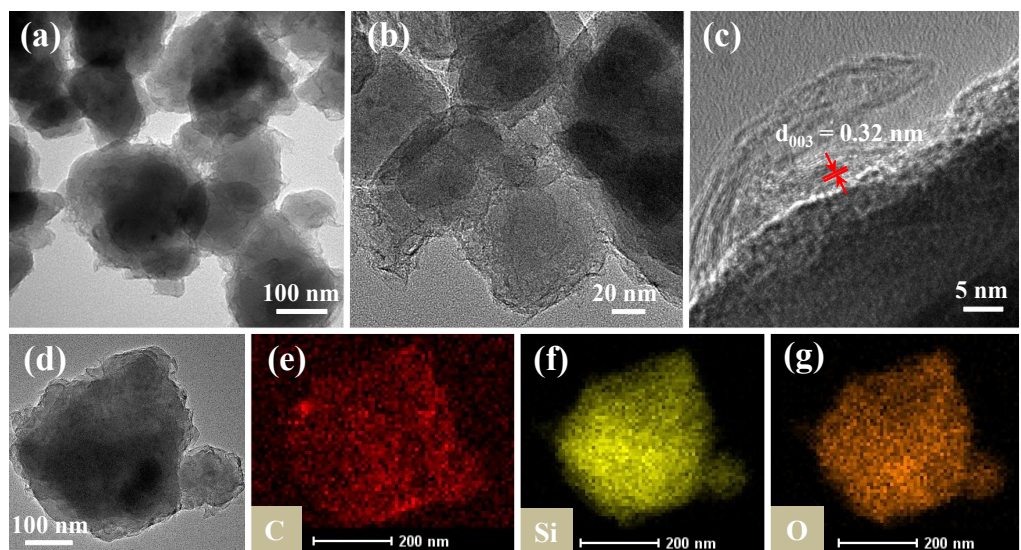


Figure S2. (a,b) TEM images and (c) high-resolution TEM image of $\text{SiO}_x@\text{G}$. (d-g) TEM image and EDS elemental mapping images of C, Si, and O of $\text{SiO}_x@\text{G}$.

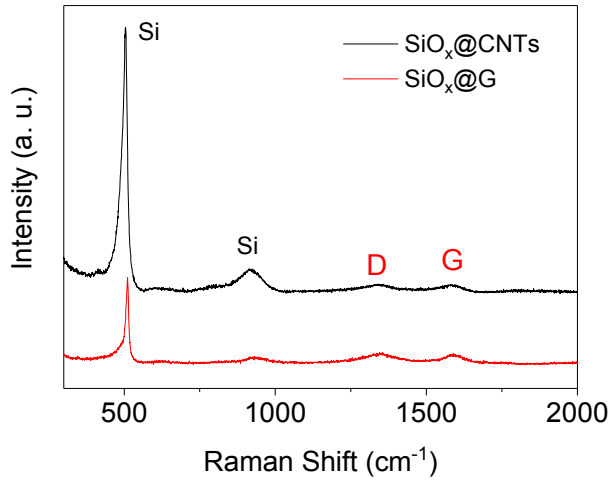


Figure S3. Raman spectra of $\text{SiO}_x@\text{CNTs}$ and $\text{SiO}_x@\text{G}$.

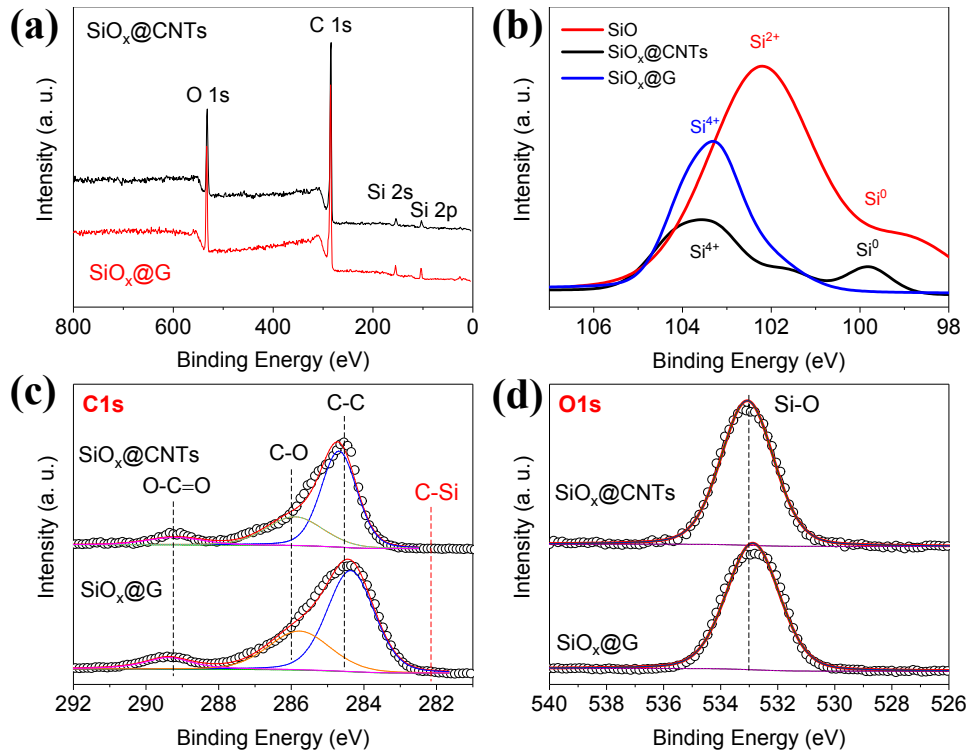


Figure S4. (a) XPS survey spectra of $\text{SiO}_x@\text{CNTs}$ and $\text{SiO}_x@\text{G}$. High resolution XPS spectra of (b) Si2p/Si2s, (c) C1s, and (d) O1s of $\text{SiO}_x@\text{CNTs}$ and $\text{SiO}_x@\text{G}$.

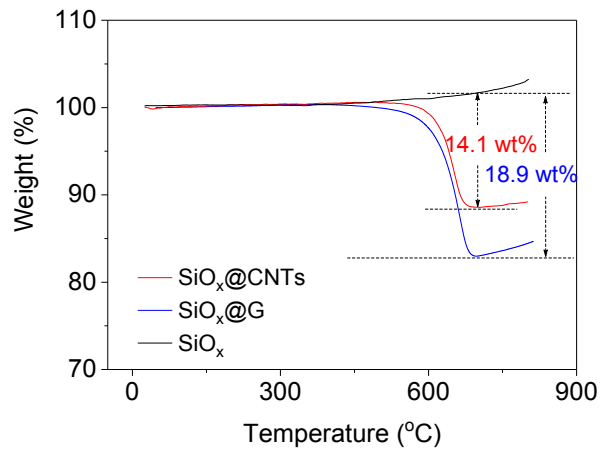


Figure S5. TGA profiles of $\text{SiO}_x@\text{CNTs}$, $\text{SiO}_x@\text{G}$ and SiO_x .

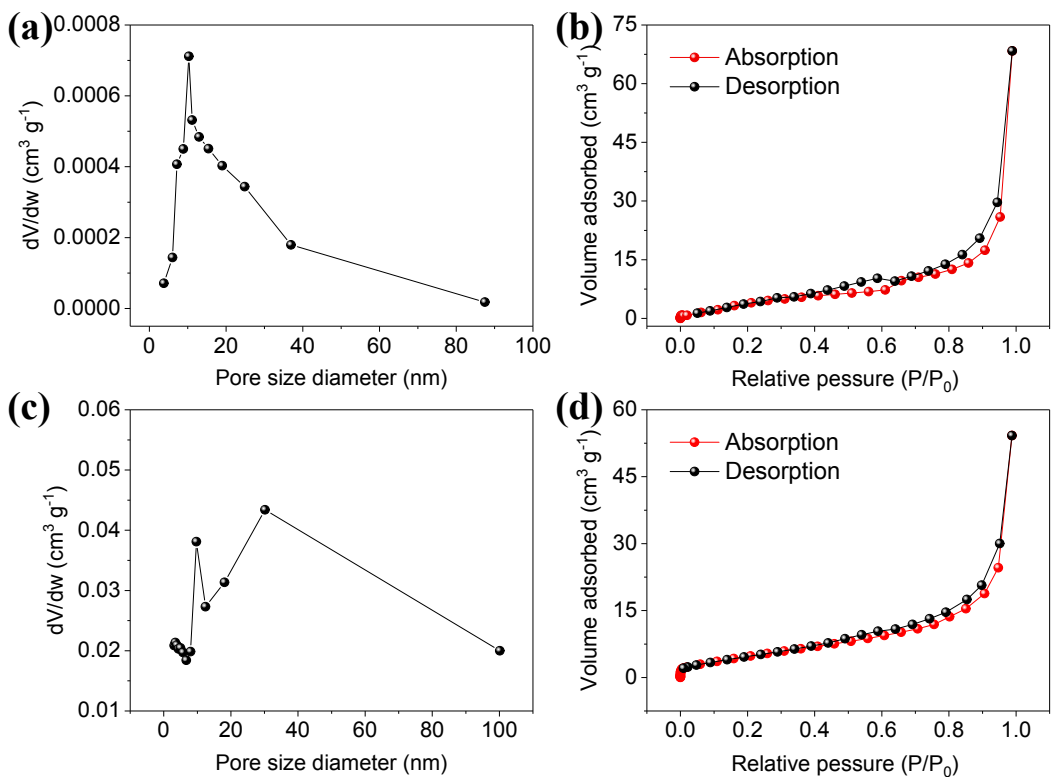


Figure S6. N₂ adsorption/desorption isotherms and pore size distribution curves of (a,b) SiO_x@CNTs and (c,d) SiO_x@G.

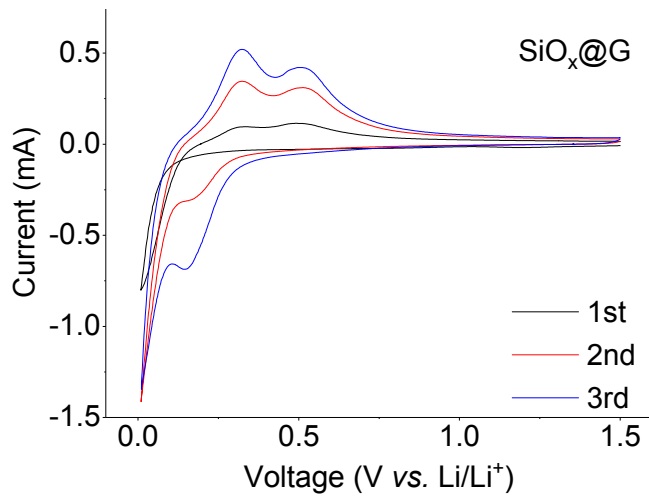


Figure S7. CV curves of $\text{SiO}_x@\text{G}$ at a scan rate of 0.1 mV s^{-1} .

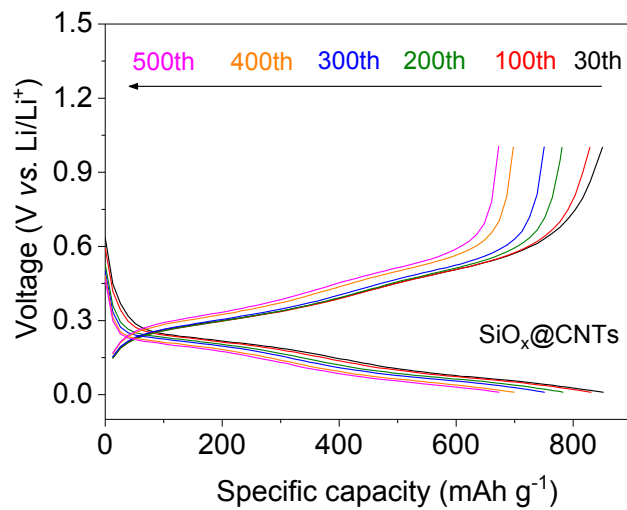


Figure S8. Typical voltage vs. capacity profiles of $\text{SiO}_x@\text{CNTs}$ in the cycle test.

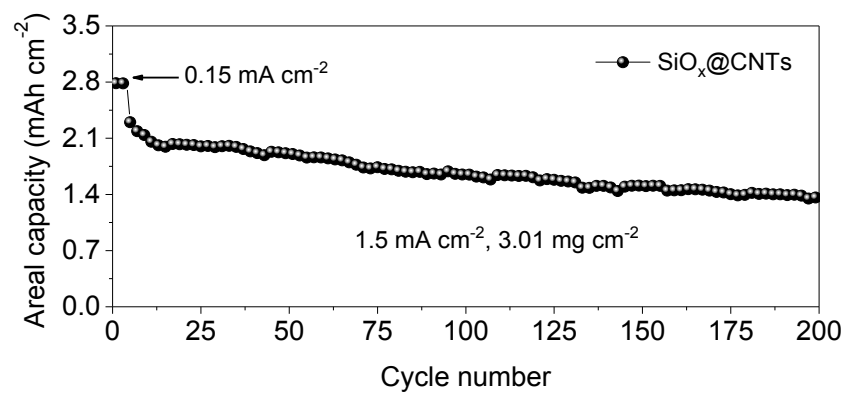


Figure S9. Cycle performance of $\text{SiO}_x@\text{CNTs}$ at a current density of 1.5 mA cm^{-2} .

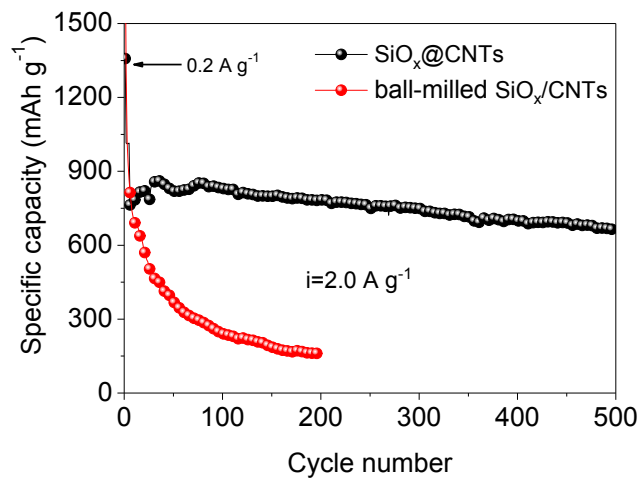


Figure S10. Comparative cycle performance of the $\text{SiO}_x@\text{CNTs}$ and ball-milled SiO_x/CNTs at a current density of 2 A g^{-1} .

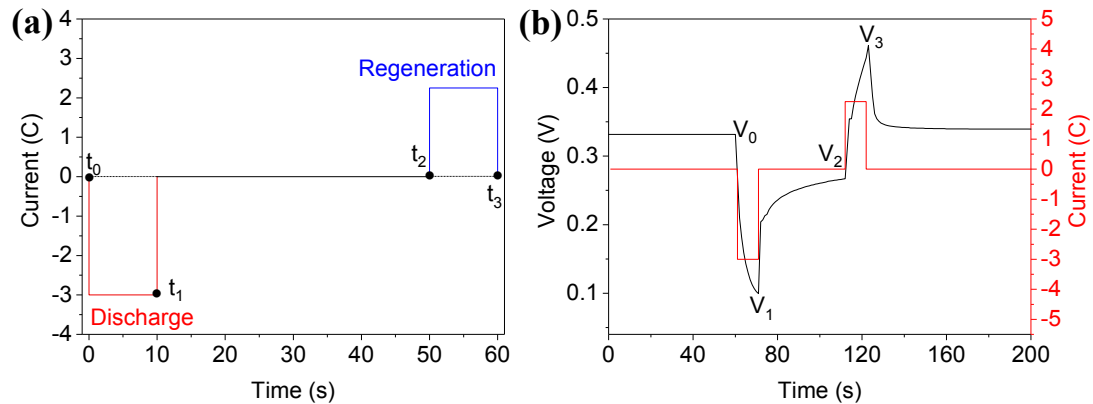


Figure S11. Method of the HPPC test. (a) The battery was pulse discharged for 10 s at a rate of 3 C, which was subsequently relaxed at the open-circuit voltage (OCV) for 40 s, and then charged for 10 s with a regenerative pulse at 75% current (2.25 C rate) of the discharge pulse. The discharge procedure was repeated from 10 to 90% depth of discharge (DOD), which was followed by a 1 h rest period before applying the next sequence. (b) One sequence under 20% DOD.

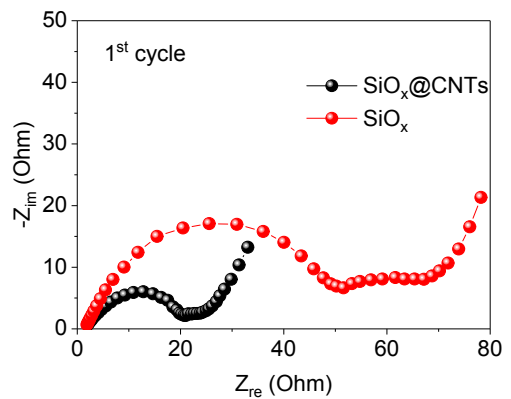


Figure S12. Nyquist plots of $\text{SiO}_x@\text{CNTs}$ and SiO_x electrodes after the 1st cycle.

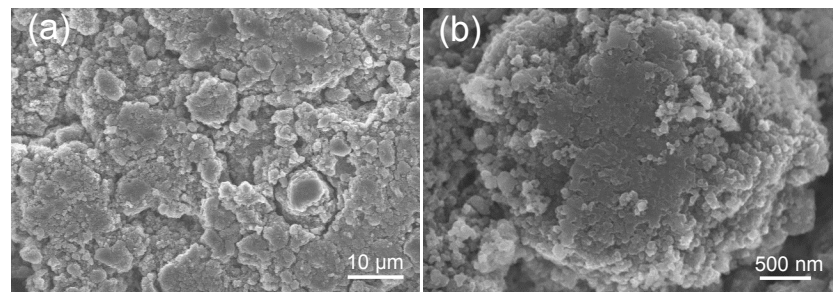


Figure S13. Ex-situ SEM images of $\text{SiO}_x@\text{G}$ anode after 100 cycles.

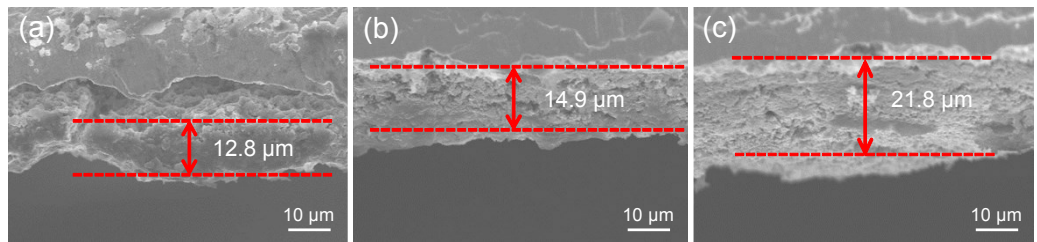


Figure S14. Cross-sectional SEM images of (a) electrode before cycling, and (b) SiO_x and (c) $\text{SiO}_x@\text{CNTs}$ electrodes after 100 cycles.

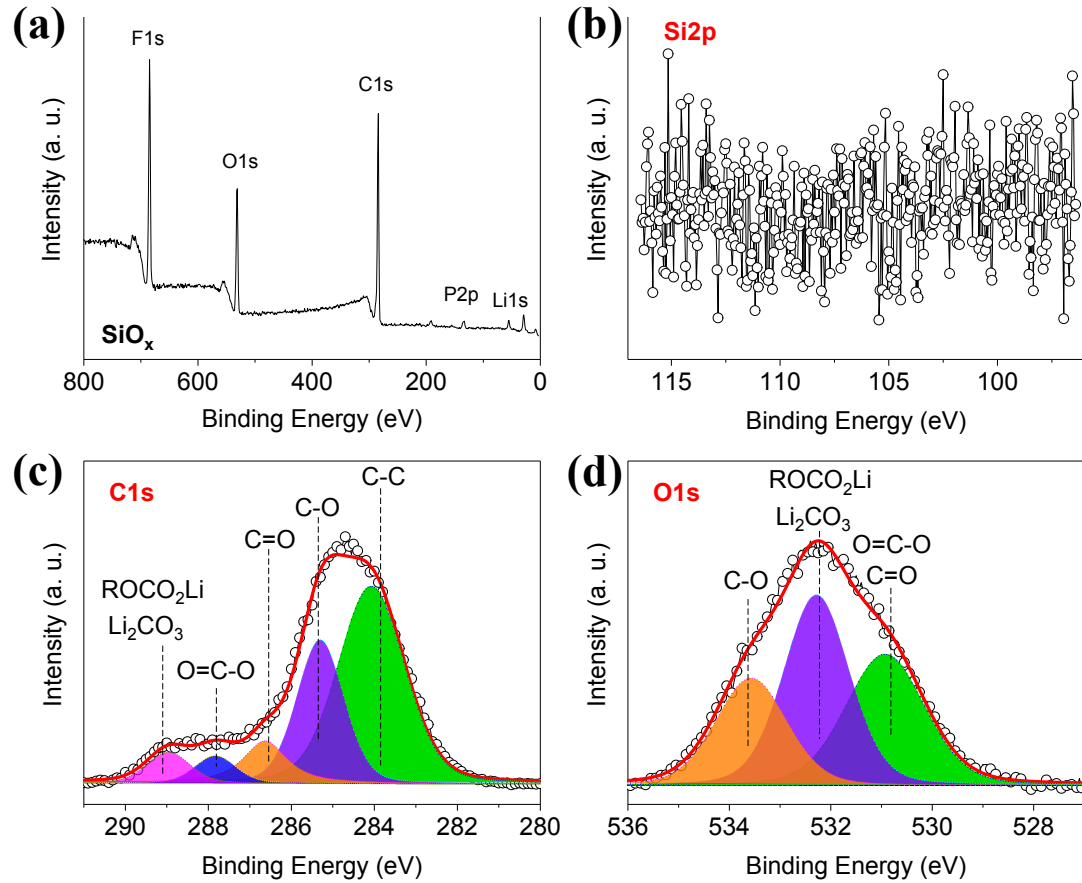


Figure S15. Surface layer characterization of the SiO_x electrode after 100 cycles. (a) Full XPS spectrum and XPS expanded spectra of (b) Si2p, (c) C1s, and (d) O1s.

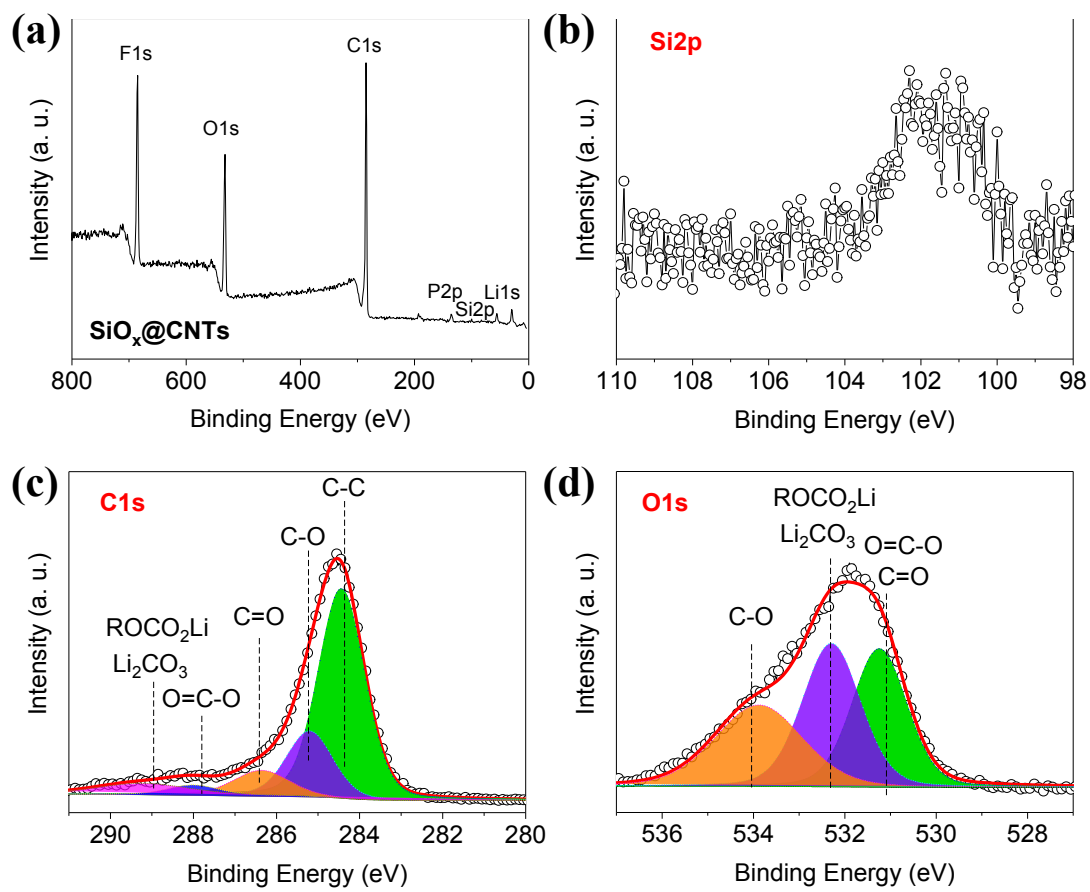


Figure S16. Surface layer characterization of the $\text{SiO}_x@\text{CNTs}$ electrode after 100 cycles. (a) Full XPS spectrum and XPS expanded spectra of (b) Si2p, (c) C1s, and (d) O1s.

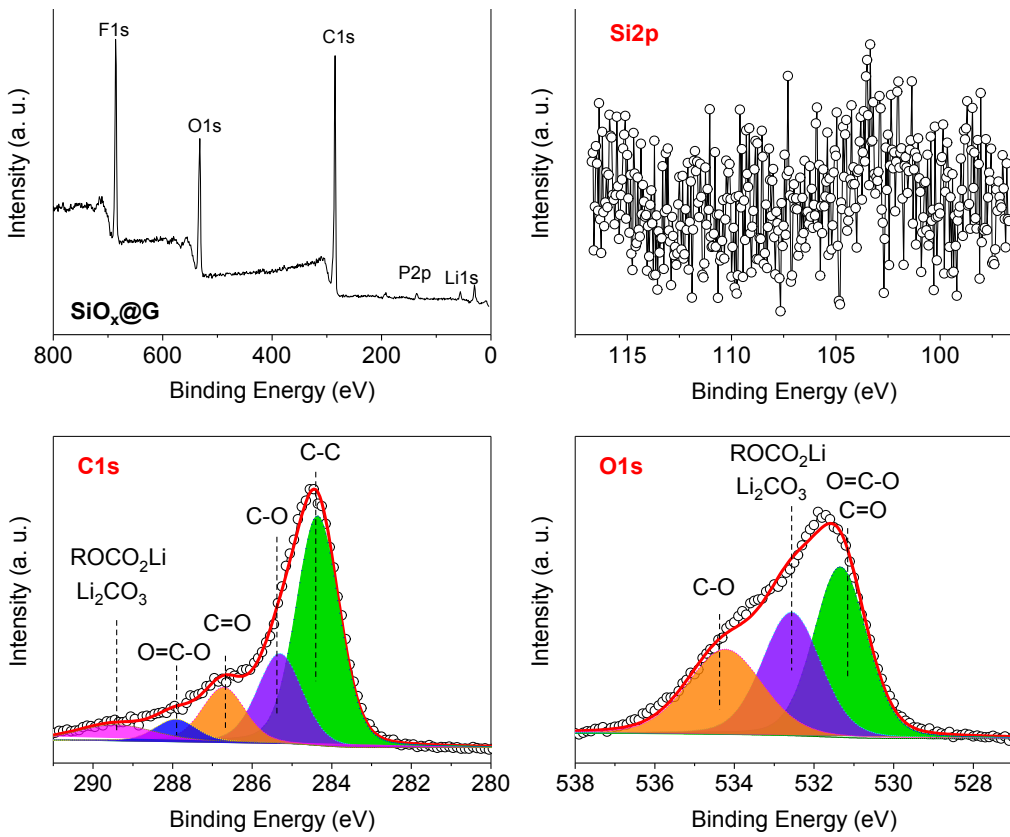


Figure S17. Surface layer characterization of the $\text{SiO}_x@\text{G}$ electrode after 100 cycles. (a) Full XPS spectrum and XPS expanded spectra of (b) Si2p, (c) C1s, and (d) O1s.

Table S1. Comparative electrochemical performance of the as-prepared $\text{SiO}_x @\text{CNTs}$ and those of the SiO_x -based composites reported previously.

Materials	Current density (A g ⁻¹)	Cycle numbers	Capacity (mAh g ⁻¹)	Retention	Ref.
$\text{SiO}_x/\text{G/C}$	0.12	500	487	74.6%	[1]
SiO_x/C spheres	1	400	493	80.9%	[2]
VG@ SiO_x/NC	2	500	642	84.2%	[3]
SiO/Sn	0.2	100	850	60.0%	[4]
YS- $\text{SiO}_x/\text{C}@\text{C}$	0.5	1000	557	76.4%	[5]
SiO_x-C	0.1	100	674	83.5	[6]
p- $\text{SiO}_x@/\text{TiO}_2@\text{C}$	0.7	500	588	61.1%	[7]
$\text{SiO}_x@/\text{CNTs}$ composites	2	500	673	89.1	This work

The energy density of the full cell is calculated by the following equation:

$$\text{Energy Density} = \frac{C_{\text{cathode}} \times C_{\text{anode}}}{C_{\text{cathode}} + C_{\text{anode}}} \times V_{\text{nominal}}$$

where C_{cathode} , C_{anode} , and V_{nominal} are 173 mAh g⁻¹, 1012 mAh g⁻¹, and 3.4 V respectively.

For example, the energy density of the full cell at 0.3 C is:

$$\text{Energy Density} = \frac{173 \text{ mAh g}^{-1} \times 1012 \text{ mAh g}^{-1}}{173 \text{ mAh g}^{-1} + 1012 \text{ mAh g}^{-1}} \times 3.4 \text{ V} = 502.3 \text{ Wh kg}^{-1}$$

References

- [1] G. Li, J.-Y. Li, F.-S. Yue, Q. Xu, T.-T. Zuo, Y.-X. Yin, Y.-G. Guo, *Nano Energy* 60 (2019) 485–492.
- [2] M. Han, J. Yu, *J. Power Sources* 414 (2019) 435–443.
- [3] M. Han, Y. Mu, F. Yuan, J. Liang, T. Jiang, X. Bai, J. Yu, *J. Mater. Chem. A* 8 (2020) 3822–3833.
- [4] R. Fu, Y. Wu, C. Fan, Z. Long, G. Shao, Z. Liu, *Chemsuschem* 12 (2019) 3377–3382.
- [5] Y. Zhang, G. Hu, Q. Yu, Z. Liu, C. Yu, L. Wu, L. Zhou, L. Mai, *Mater. Chem. Front.* 4 (2020) 1656–1663.
- [6] W. Wu, J. Shi, Y. Liang, F. Liu, Y. Peng, H. Yang, *Phys. Chem. Chem. Phys.* 17 (2015) 13451–13456.
- [7] F. Dou, Y. Weng, G. Chen, L. Shi, H. Liu, D. Zhang, *Chem. Eng. J.* 387 (2020) 124106.